

Identifying discontinuities of flood frequency curves

Arianna Miniussi¹, Ralf Merz¹, Lisa Kaule^{1,2}, Stefano Basso¹

¹Department of Catchment Hydrology, Helmholtz Centre for Environmental Research - UFZ, Halle
(Saale), Germany

²Institute of Geosciences and Geography, Martin-Luther University Halle-Wittenberg, Halle (Saale),
Germany

³Department of Hydrology, University of Bayreuth, Bayreuth, Germany

Highlights:

- We develop an automated method to detect discontinuities of flood frequency curves
- We test it on observed and physically-based theoretical flood frequency curves
- We discuss the reliability of the physically-based approach to detect discontinuities

Corresponding author: Stefano Basso, stefano.basso@ufz.de

Abstract

Discontinuities in flood frequency curves, here referred to as flood divides, hinder the estimation of rare floods. In this paper we develop an automated methodology for the detection of flood divides from observations and models, and apply it to a large set of case studies in the USA and Germany. We then assess the reliability of the PHysically-based Extreme Value (PHEV) distribution of river flows to identify catchments that might experience a flood divide, validating its results against observations. This tool is suitable for the identification of flood divides, with a high correct detection rate especially in the autumn and summer seasons. It instead tends to indicate the emergence of flood divides not visible in the observations in spring and winter. We examine possible reasons of this behavior, finding them in the typical streamflow dynamics of the concerned case studies. By means of a controlled experiment we also re-evaluate detection capabilities of observations and PHEV after discarding the highest maxima for all cases where both empirical and theoretical estimates display flood divides. PHEV mostly confirms its capability to detect a flood divide as observed in the original flood frequency curve, even if the shortened one does not show it. These findings prove its reliability for the identification of flood divides and set the premises for a deeper investigation of physiographic and hydroclimatic attributes controlling the emergence of discontinuities in flood frequency curves.

1 Introduction

Despite considerable efforts to achieve reliable estimation of rare floods, these events are still among the most common natural disasters (Wallemacq & House, 2018). The evaluation of their hazard is however crucial for several applications, including the design of hydraulic structures, risk planning and mitigation, and computation of premiums in the insurance industry. Appraisal of the flood hazard is especially difficult when the magnitude of the rarer floods can take values which are several times to orders of magnitude larger than commonly observed floods, resulting in a marked uprise of the flood frequency curve beyond certain return periods (Rogger et al., 2012; Smith et al., 2018).

Cognitive biases often lead to downplay the occurrence of such extreme events (B. Merz et al., 2015, 2021), although the scientific literature repeatedly signalled the pervasiveness of these behaviors terming them in various ways. In fact, heavy-tailed distributions of floods (Farquharson et al., 1992; Bernardara et al., 2008; Villarini & Smith, 2010), inversions of

43 concavity and step changes in flood magnitude-frequency curves (Rogger et al., 2012; Guo
44 et al., 2014; Basso et al., 2016) and large values of the ratios between the maximum flood of
45 record and the sample flood with a specified recurrence time (Smith et al., 2018) and between
46 empirical high flow percentiles (Mushtaq et al., 2022) are all manifestations of a marked
47 increase of the magnitude of the rarer floods highlighted by means of different approaches.
48 To further stress the common nature of all these phenomena, in this study we favor none
49 of the previous locutions and instead label them as *flood divides*. The term was chosen to
50 highlight the existence of a discharge threshold which marks the rise of progressively larger
51 floods (red square in Figure 1d) and thus distinguishes between common and increasingly
52 extreme floods that may occur in river basins.

53 Rogger et al. (2012) investigated marked uprisings (i.e., discontinuities in the slope) of
54 flood frequency curves, which they called step changes, by leveraging information collected
55 from field surveys in two small alpine catchments to calibrate a distributed deterministic
56 rainfall-runoff model. They suggested that step changes occur when a threshold of the
57 catchment storage capacity is exceeded, and performed a synthetic experiment (Rogger et al.,
58 2013) to examine the effect of catchment storage thresholds and combined multiple controls
59 (e.g., the temporal variability of antecedent soil storage and the size of the saturated regions)
60 on the return period of the step change. They also highlighted important implications of the
61 presence or absence of flood divides for estimation and design purposes, further stressing the
62 need for a robust method to identify their possible occurrence. In fact, misidentifying the
63 presence of flood divides may either lead to overestimation of rare floods (if large recorded
64 outliers are considered in the analyses) or to their underestimation, in case events larger
65 than the flood divide were not yet recorded or are regarded as outliers.

66 Guo et al. (2014) and Basso et al. (2016) instead linked different shapes of flood fre-
67 quency curves and a marked growth of the magnitude of the rarer floods to the catchment
68 water balance. The former justified these features through the aridity index (i.e., the ra-
69 tio between mean annual potential evaporation and precipitation, Budyko (1974)), showing
70 that flood frequency curves characterized by increasing aridity index are steeper. The latter
71 explained them by means of the persistency index (i.e., the ratio between mean catchment
72 response time and runoff frequency, Botter et al. (2013)) and highlighted that the concavity
73 of the flood frequency curve changes from downward to upward shifting from persistent to
74 erratic regimes, thus causing the emergence of flood divides.

75 Smith et al. (2018) computed the ratio between the maximum flood of record and the
76 sample 10-year flood for thousands of gauges across the USA, finding large values for a
77 substantial amount of them. Different flood-generating processes (R. Merz & Blöschl, 2003;
78 Berghuijs et al., 2014; Tarasova et al., 2020) or mixtures of flood event types (Hirschboeck,
79 1987; Villarini & Smith, 2010; Smith et al., 2018) were indicated by other studies as possible
80 causes of these marked increases of the magnitude of the rarer floods.

81 Finally, a rather common approach to study this phenomenon consists in evaluating
82 the shape parameter of Generalized Extreme Value distributions fitted to observed annual
83 maximum series (Farquharson et al., 1992; Bernardara et al., 2008; Villarini & Smith,
84 2010; Smith et al., 2018). Notwithstanding the drawbacks of such a parametric approach
85 applied in association with limited records of annual maxima, these studies highlighted the
86 ubiquitous occurrence of flood divides and flood distributions characterized by thick upper
87 tails, as indicated by widespread positive values of the shape parameter. Moreover, Smith et
88 al. (2018) showed that the values of the shape parameter significantly increase with longer
89 data records. Their findings thus suggest that uprisings of flood frequency curves may be the
90 norm rather than rare conditions, pointing to the limited data record as the reason for the
91 latter belief.

92 Although former research hints at the ubiquitousness of flood divides in flood frequency
93 curves and provide indications of their possible drivers, a quantitative methodology to iden-
94 tify flood divides, which is robust to sampling uncertainty and tested in a large set of case
95 studies, is still lacking. The relevance of our study is thus twofold: (i) we develop such a
96 methodology for the detection of flood divides and evaluate their emergence across the US
97 and Germany, in a large set of catchments with contrasting physio-climatic features; (ii) we
98 examine the reliability of a process-based stochastic framework for the estimation of flood
99 frequency curves to detect flood divides and infer their occurrence, benchmarking its results
100 against observations.

2 Methodology and Data

2.1 The Physically-based Extreme Value distribution of river flows

2.1.1 Theoretical framework

The Physically-based Extreme Value (PHEV) distribution of river flows is a parsimonious mechanistic-stochastic formulation of flood frequency curves (Basso et al., 2016, 2021) that stems from a rigorous mathematical description of catchment-scale daily soil moisture and streamflow dynamics in river basins (Laio et al., 2001; Porporato et al., 2004; Botter et al., 2007). In this framework, daily precipitation is represented as a marked-Poisson process with frequency $\lambda_P [T^{-1}]$ and exponentially-distributed depths with average value $\alpha [L]$. Soil moisture decreases due to evapotranspiration and is replenished by precipitation events that eventually trigger runoff pulses when an upper wetness threshold is crossed. These pulses, which feed water to a hydrologic storage, are also a Poisson process with frequency $\lambda < \lambda_P$ $[T^{-1}]$ and an exponential distribution of magnitudes with mean $\alpha [L]$. A non-linear (i.e., power-law) storage-discharge relation with parameters a and K epitomizes the hydrological response of the catchment and encompasses the joint effect of different flow components (Brutsaert & Nieber, 1977; Basso, Schirmer, & Botter, 2015).

The above-summarized mechanistic-stochastic description of runoff generation processes allows for expressing the probability distributions of daily flows (Botter et al., 2009) and peak flows (i.e., local flow peaks occurring as a result of streamflow-producing rainfall events) as a function of a few physically meaningful parameters (Basso et al., 2016). It also enables characterizing hydrologic regimes according to their typical streamflow dynamics, which are summarized by the persistency index (Botter et al., 2013). This is defined as the ratio between runoff frequency and the mean hydrograph recession rate, i.e., $\frac{\lambda}{K(\alpha\lambda)^{a-1}}$ (Basso et al., 2016; Deal et al., 2018).

An erratic regime (lower values of the persistency index), which is commonly found during dry seasons, very hot humid seasons with intense evapotranspiration or in fast responding catchments, is characterized by periods between the arrival of runoff-producing rainfall events which are longer than the typical duration of flow pulses. Conversely, a persistent regime (higher values of the persistency index), typically occurring in cold-humid seasons and lowland catchments, is characterized by frequent rainfall events and a rather constant water supply to the catchment.

132 Considering that peak flows in a given reference period (e.g., a season) are Poisson
 133 distributed and postulating their independence yield the probability distribution of flow
 134 maxima (i.e., maximum values in a specified timespan). The return period is finally obtained
 135 as the inverse of the exceedance cumulative probability of flow maxima, thus providing an
 136 expression of the flood frequency curve which reads (Basso et al., 2016):

$$T_r(q) = \frac{1}{1 - \exp[-\lambda\tau D_j(q)]} \quad (1)$$

137 where τ [T] is the duration in days of the reference period used in the analyses; $D_j(q) =$
 138 $\int_q^\infty p_j(q) dq$ is the exceedance cumulative probability of peak flows; p_j is the probability
 139 density function of peak flows, $p_j(q) = Cq^{1-a} \exp(\frac{\lambda q^{1-a}}{K(1-a)} - \frac{q^{2-a}}{\alpha K(2-a)})$; α and λ are the
 140 aforementioned parameters describing Poisson-distributed runoff events, a and K are the
 141 parameters of the power-law storage-discharge relation, and C is a normalization constant.

142 **2.1.2 Parameter Estimation**

143 The four parameters of PHEV (α , λ , a , K) are rather straightforward to estimate
 144 at the catchment scale. They are indeed directly derived from the observed time series
 145 of precipitation and streamflow: α is computed as the mean daily rainfall depth in rainy
 146 days, while λ (frequency of streamflow-producing rainfall) as the ratio between the long
 147 term mean daily flow $\langle q \rangle$ and α (Botter et al., 2007). The parameters of the power-law
 148 storage-discharge relation (i.e., the recession exponent a and coefficient K) are estimated
 149 through hydrograph recession analysis (Brutsaert & Nieber, 1977) following the approach
 150 proposed by Biswal and Marani (2010). Finally, the recession coefficient is not directly used
 151 as input in Eq. (1), but it is replaced by its maximum likelihood estimation on the observed
 152 seasonal flood frequency curve (Basso et al., 2016).

153 **2.2 Identification of Flood Divides**

154 To identify flood divides, we start from the method proposed by Rogger et al. (2013): a
 155 flood divide is defined as the sharpest bend of the flood frequency curve, here considered in
 156 terms of rescaled streamflow maxima (i.e., seasonal maxima divided by the long term mean
 157 daily flow, $\langle q \rangle$) as a function of the return period, the latter represented in logarithmic
 158 scale. We then develop a new methodology dedicated to its identification from both empirical
 159 estimates of the flood frequency curve obtained by means of Weibull plotting position and

160 models, such as PHEV. The resulting approach, which can be employed without depending
161 on subjective evaluation, is detailed in the following.

- 162 1. The curvature of the flood frequency curve, of which we show an example in Figure
163 1, is computed as $\log Tr'' / (1 + \log Tr'^2)^{(3/2)}$ (where the apex indicates the derivation
164 operation with respect to the rescaled streamflow) for both the observations and
165 PHEV. In the former case, we use the method developed by Jianchun et al. (1994)
166 for computing derivatives in non-equally spaced points, while for PHEV we employ
167 the Python routine from the Scipy library (*misc.derivative*), which uses a central
168 difference formula with spacing dx to compute the n^{th} derivative at a specified point.
- 169 2. As the noise associated to computing the curvature on a discrete and rather sparse
170 set of points (seasonal maxima) might lead to identification errors, a heuristic filter is
171 applied on the curvature calculated from observations: only points on the right-hand
172 side of the last value of the curvature exceeding the range $\pm\sigma$ (where σ indicates the
173 standard deviation of the curvature itself) are considered (Figure 1c);
- 174 3. The Mann-Whitney U-test (Mann & Whitney, 1947) is applied on the values of the
175 first derivatives on the left and right-hand sides of each potential flood divide identified
176 at point 2 to check if their distributions are statistically different at a significant level
177 equals to 0.05 (in other words, if the slope of the curve significantly differs between
178 the left and right-hand side of the flood divide); the effect size is then computed by
179 means of the Cohen's d (Cohen, 1974) to evaluate if the magnitude of the difference is
180 relevant (Sullivan & Feinn, 2012). For PHEV, this step is performed on a dense set of
181 values, equally spaced with an interval $\Delta q = 0.05$ up to a value of rescaled streamflow
182 equal to 200, i.e., 200 times the long-term average streamflow. The relative increment
183 of the slope between the left and right-hand side of a potential PHEV flood divide is
184 also evaluated within the observational range.
- 185 4. We finally identify as flood divide the point for which the p-value of the Mann-
186 Whitney test is the lowest, provided that the Cohen's d is greater than 0.4 (moderate
187 effect size; Gignac and Szodorai (2016); Lovakov and Agadullina (2021)) and the slope
188 increment exceeds a value of 1%.

189 Figure 1 visually exemplifies the application of the developed approach for flood divides
190 detection to the flood frequency curve of the Rott river at Kinning, Bavaria (ID: 18801005),
191 in the summer season. In Figure 1a the flood frequency curve is represented with switched

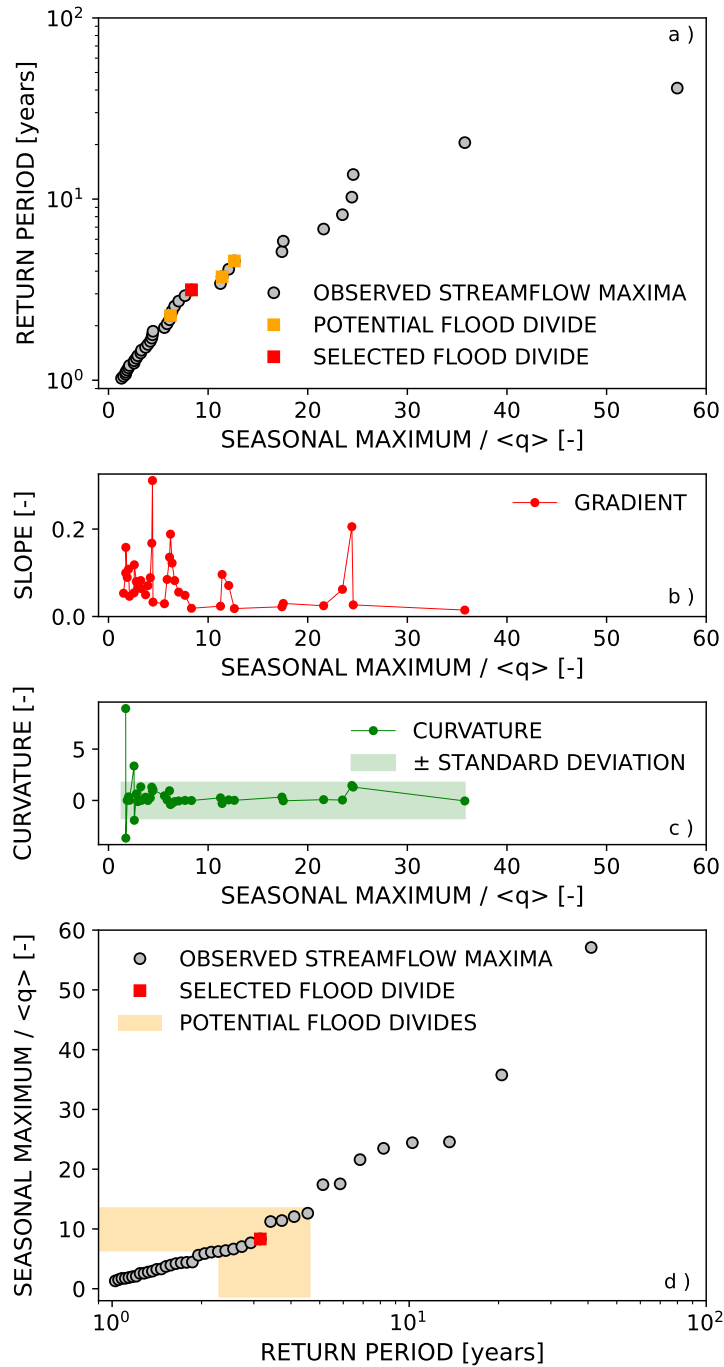


Figure 1: Exemplary application of the proposed methodology to detect flood divides to the Rott river at Kinning, Bavaria (ID: 18801005), in the summer season. a) Visualization of how the approach is actually applied, i.e., expressing the logarithm of the return period as a function of the rescaled seasonal maxima (gray filled circles). Potential flood divides (i.e., all the points with a p-value of the Mann-Whitney U-test lower than 0.05) are represented by orange squares, while the selected one (i.e., the one exhibiting the minimum p-value of the Mann-Whitney U-test and Cohen's d greater than 0.4) is depicted with a red square. b) First derivative computed on observations. c) Curvature computed on observations, with the shaded area representing twice its standard deviation. d) Standard representation of the flood frequency curve, namely observed maxima as a function of the logarithmic value of the return period (gray filled circles). The red square indicates the selected flood divide, while the orange shaded area represents the range of potential flood divides.

192 axes (i.e., the logarithm of the return period is represented on the y-axis whereas the rescaled
193 seasonal maxima on the x-axis), as streamflow is the independent variable in Eq. (1). The
194 red square in Figure 1a,d represents the selected flood divide, i.e., the one associated to
195 the lowest p-value of the Mann-Whitney U-test applied to the distributions of the first
196 derivatives (Figure 1b) and fulfilling the additional criterion on the Cohen's d . We also
197 show points that are initially analyzed as potential flood divides (i.e., all the points with a
198 Mann-Whitney p-value lower than 0.05, orange squares in Figure 1a).

199 2.3 Datasets

200 We use daily rainfall and streamflow time series from the Model Parameter Estimation
201 Experiment dataset (MOPEX, data from 1948 to 2003) (Duan et al., 2005; Schaake et
202 al., 2006) and from Germany (1951-2013) (Tarasova et al., 2018). Streamflow is measured
203 at the gauging stations whose geographical coordinates are listed in Table S1, whereas
204 the corresponding rainfall records are spatially averaged values for the upstream drainage
205 areas derived from gridded datasets. We perform all analyses in a seasonal time frame
206 (spring: March to May; summer: June to August; autumn: September to November; winter:
207 December to February) to account for the seasonality of rainfall and runoff (Allamano et
208 al., 2011; Baratti et al., 2012). To assure that PHEV suitably represents the key processes
209 of streamflow generation in the set of case studies, we only consider catchments with low
210 human impact, weak or absent inter-seasonal snow dynamics (Botter et al., 2013; Wang
211 & Hejazi, 2011) and hydrograph recession properties which are independent of the peak
212 flow (Basso et al., 2021). Similarly to previous studies (R. Merz et al., 2020), we as well
213 restrict our analysis to cases for which the root mean square error ($RMSE$) between the
214 predicted and observed flood frequency curve is limited (i.e., lower than 0.3), as a fairly
215 accurate estimation of the flood frequency curve is a precondition to investigate if PHEV is
216 able to correctly identify flood divides and whether their occurrence is affected by physio-
217 climatic catchment attributes. Figure S1 provides a summary of the performance of PHEV
218 (quantified by means of varied error metrics, see Supplementary Material) in reproducing
219 observed flood frequency curves in the considered set of case studies. This selection yields a
220 set of 101 case studies (i.e., catchment-season combinations), divided into 23, 29, 23 and 26
221 cases respectively in the spring, summer, autumn and winter seasons. The median length
222 of the considered data series is 54 years (min: 34, max: 55) for the MOPEX and 58 years

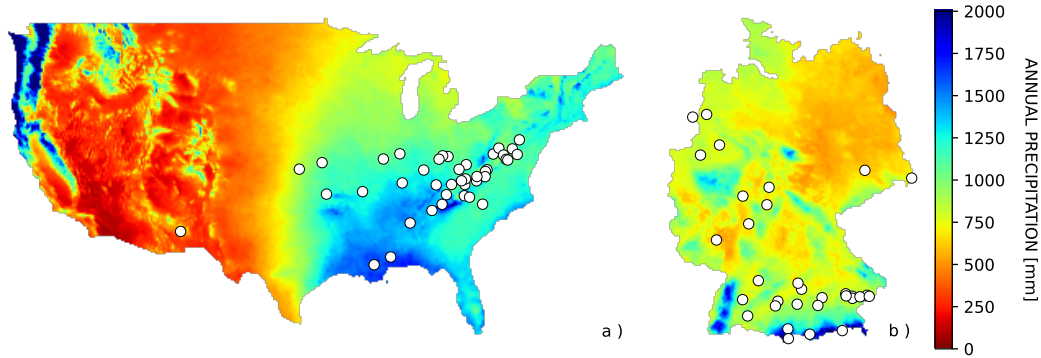


Figure 2: Select river basins (white filled circles) from the (A) MOPEX and (B) German datasets. The background of the maps represents 30-years annual precipitation normals (1981-2010 for the US and 1991-2020 for Germany).

223 (min: 40, max: 63) for the German case studies. Their catchment areas vary between 43
 224 and 9052 km² (median: 865 km²). The locations of their outlets are displayed in Figure 2.

225 3 Results and Discussion

226 We apply the methodology for the identification of flood divides introduced in the
 227 previous section to each observed and analytic seasonal flood frequency curve, thus allowing
 228 for evaluating the flood divide detection of PHEV against observations, which we consider
 229 as benchmark (Figure 3). The bar plots in Figure 3 show the percentages of case studies
 230 for which a flood divide is identified from both PHEV and the observational records (true
 231 positives, dark green color), those which display a flood divide neither in the empirical nor
 232 in the analytic flood frequency curves (true negatives, light green), the percentages of cases
 233 where a flood divide is detected from the observations but not from the analytical model
 234 (false negatives, red), and those where the analytical model has foreseen the occurrence of
 235 a flood divide which is not confirmed by the available observations (false positives, orange).
 236 The existence of both true positives and true negatives emphasizes the capability of PHEV
 237 to mimic varied observed shapes of flood frequency curves (Basso et al., 2016) and to identify
 238 both the presence and the absence of a flood divide.

239 The bar plots in Figure 3a and 3b differ for the criteria applied in the flood divide iden-
 240 tification methodology. In Figure 3a only the controls on the p-value of the Mann-Whitney
 241 U-test mentioned in Section 2.2 are considered, whereas the additional requirements on the
 242 effect size and slope increment are as well used in Figure 3b. True positives (dark green)

243 prevail in the summer (18 cases) and autumn (14 cases) seasons of Figure 3a, amounting
244 to about 60% of the cases. False positives constitute instead a sizable share of the cases in
245 spring (12 cases) and winter (21 cases). When more stringent requirements for the identi-
246 fication of flood divides are used, by accounting for the mentioned additional criteria, the
247 percentage of true positives decreases (Figure 3b, dark green; respectively 3, 11, 12 and 1
248 cases in spring, summer, autumn and winter). A few cases of those shifting category be-
249 come true negatives (for an overall number of 2, 3, 1 and 1 cases in spring, summer, autumn
250 and winter), indicating that the slope of the flood frequency curve does not substantially
251 increases on the right-hand side of the potential flood divide, thus not representing a note-
252 worthy hazard. Most of them however become false positives (orange color in Figure 3b;
253 respectively 18, 15, 9 and 24 cases in spring, summer, autumn and winter) as the identified
254 changes of the slope of the observed flood frequency curve are not substantial according to
255 the limited amount of available observations, whereas PHEV confirms the existence of a
256 flood divide thanks to its evaluation in an unlimited number of points. Consistent results
257 are also found when considering different significant levels for the Mann-Whitney test: the
258 strictest the level the highest the share of cases shifting between true and false positives,
259 which once again points to the unfeasibility of detecting flood divides with confidence from
260 plain observations.

261 The predominance of false positives in spring (18 cases) and winter (24 cases) (orange
262 color in Figure 3b) calls for further investigation of their causes. We therefore hypothesize
263 that PHEV, by leveraging the embedded mechanistic description of hydro-climatic dynamics
264 taking place in watersheds and the information gained from analyzing daily rainfall and
265 streamflow series, might indicate the possible emergence of flood divides that are not yet
266 displayed by the observed flood frequency curves. In fact, these empirical estimates are
267 likely affected by small sizes of the samples of large events (i.e., those on the right-hand side
268 of each potential flood divide, see Figure 1a) and by the specific character of catchments,
269 which may have a more or less enhanced propensity to exhibit extreme floods and thus
270 display them in a limited data record. We then perform the following experiment to test
271 this hypothesis. We consider the set of true positives (i.e., the 27 cases for which both
272 PHEV as well as the observed flood frequency curve show a flood divide) and retain only
273 maxima with return periods below 5 years (see an explanatory example in Figure 4a, where
274 the maxima retained are represented by gray filled circles with blue contours). In so doing,
275 we approximately discard in each case the largest ten points and their corresponding years

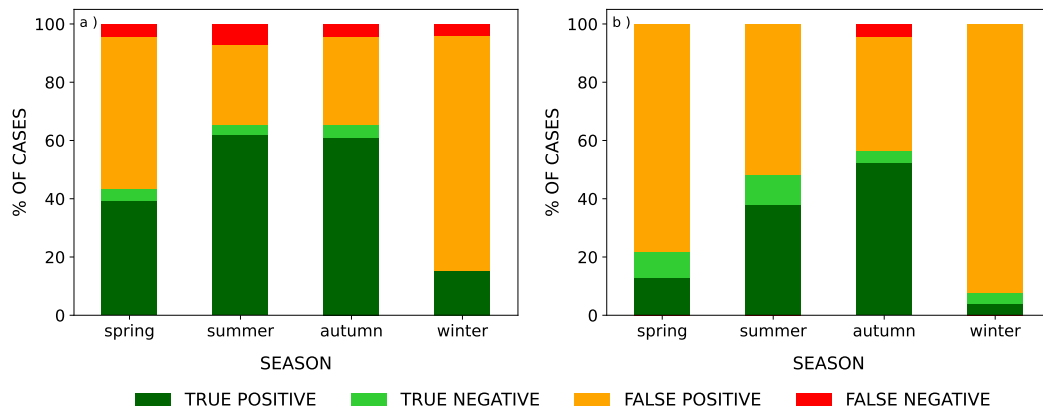


Figure 3: Performance of the PHysically-based Extreme Value (PHEV) distribution of river flows in the detection of flood divides when only the controls on the Mann-Whitney U-test are considered (see Section 2.2, panel a) and when the whole methodology for detecting flood divides is applied (see Section 2.2, panel b). Percentages are calculated on the overall number of case studies, which amount to 23, 29, 23 and 26 cases respectively in the spring, summer, autumn and winter seasons. True positives (dark green color; 27 cases in panel b) and true negatives (light green; 7 cases) indicate coherence between PHEV and observations, i.e., flood divides are either detected or not from both PHEV and the observed records. These constitute a large number of cases in summer (14 cases) and autumn (13 cases). False positives (orange; 66 cases) and false negatives (red; 1 case) represent the cases in which either PHEV detects a flood divide that was not identified by the observations or the observations display a flood divide which is not detected by PHEV. The indicated absolute numbers of positive and negative cases refer to the complete application of the methodology for detecting flood divides (i.e., panel b). The reasons for the presence of false positives are further investigated in the study and clarified in the text and figures.

276 of occurrence. Thereby, fictitious flood frequency curves only comprising maxima with
277 smaller magnitudes (and return periods) are created, thus reproducing the conditions we
278 hypothesized as possible reasons of the emergence of false positives. We then apply the
279 usual methodology for identifying flood divides on these fictitious flood frequency curves
280 and the corresponding shortened data records.

281 PHEV detects a true flood divide (i.e., true positives) in 81% of the cases (22 case
282 studies) even when the largest points are removed, whereas the observations only in 40%
283 (11 cases). The maps in Figure 4b and 4c summarize this result: half circles are colored
284 either in green, if a flood divide is successfully detected from the shortened flood frequency
285 curve, or in red in the opposite case. The left half of the circle depicts the detection
286 capability of PHEV, while the right side the results obtained from the observations. It can
287 be easily seen that most left halves of the circles are colored in green and most of the right
288 ones are instead red, thus indicating a high success rate of PHEV and a significantly lower
289 one of observations in inferring the emergence of flood divides from shortened records. A
290 similar result is obtained by discarding maxima with return period greater than 10 years
291 (i.e., discarding about five-six points instead of the highest ten), when PHEV correctly
292 detects 85% of true flood divides (23 cases) in comparison to a correct detection rate from
293 observations of 60% (16 cases). The outcome of this experiment strongly suggests that the
294 detected false positives (orange color in Figure 3) indeed arise because of the statistical
295 uncertainty of limited data records and the capability of PHEV to infer the occurrence of
296 flood divides from short series rather than by its inability to correctly identify inflection
297 points which were detected (or not) in the observed flood frequency curves.

298 A physical explanation of the reason why some observational series might not exhibit a
299 flood divide which shall be expected is provided by considering typical streamflow dynamics
300 occurring for distinct river flow regimes, here characterized by means of the persistency
301 index (Botter et al., 2013). When streamflow values weakly oscillate around their mean
302 (persistent regimes), the probability of occurrence of relatively large flows is very low, and
303 extreme events are unlikely to be captured by short time series. On the contrary, erratic
304 regimes are composed of a sequence of high flows interspersed in between prolonged periods
305 of low flows. Events which are several times (i.e., order of magnitudes) higher than the
306 average flow are thus more likely to occur in these regimes (Basso, Frascati, et al., 2015). In
307 the context of this study, false positives shall therefore mostly occur for persistent regimes,

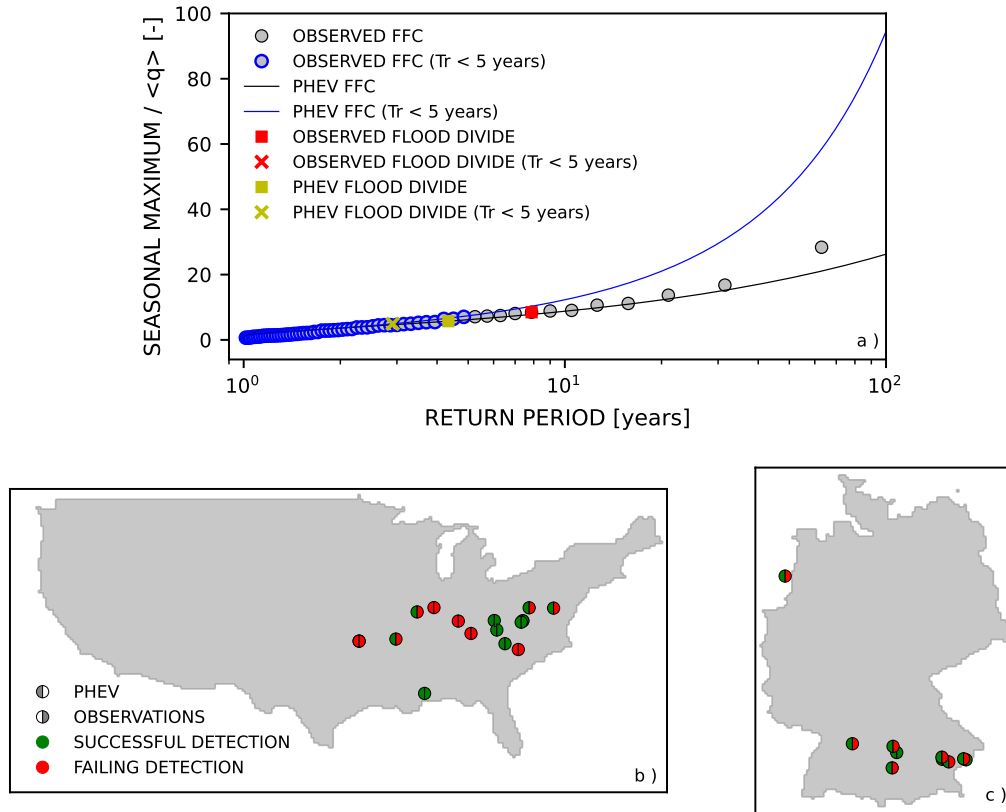


Figure 4: Visual explanation and results of an experiment aimed at testing hypotheses on the emergence of false positives. a) Gray dots with black (blue) contour represent the complete (shortened, until a return period of 5 years) observed seasonal maxima series of the Wörnitz river at Harburg, Bayern (ID:11809009), in the summer season. The solid black (blue) line displays the analytic flood frequency curve (i.e., PHEV) whose parameters are estimated from the complete (shortened) time series. The red (yellow) square indicates the flood divide detected from the observations (by PHEV) using the complete series, while the corresponding crosses (the red one is not visible in the plot as no flood divide was detected after shortening the observations) represent the observed and analytic flood divides detected on the shortened flood frequency curve. b-c) Locations of the true positives in the US (panel b) and Germany (panel c). The left (right) half of the circles represent PHEV (observations) ability to detect a flood divide when the shortened flood frequency curves (i.e., maxima characterized by return period below 5 years) are used. The green (red) colored halves indicate successful (failing) detection. Remarkably, most of the left halves are green (PHEV detects true flood divides even from the shortened series in the majority of the cases), whereas most of the right ones are red (flood divides are not always identified from observations when the shortened records are used).

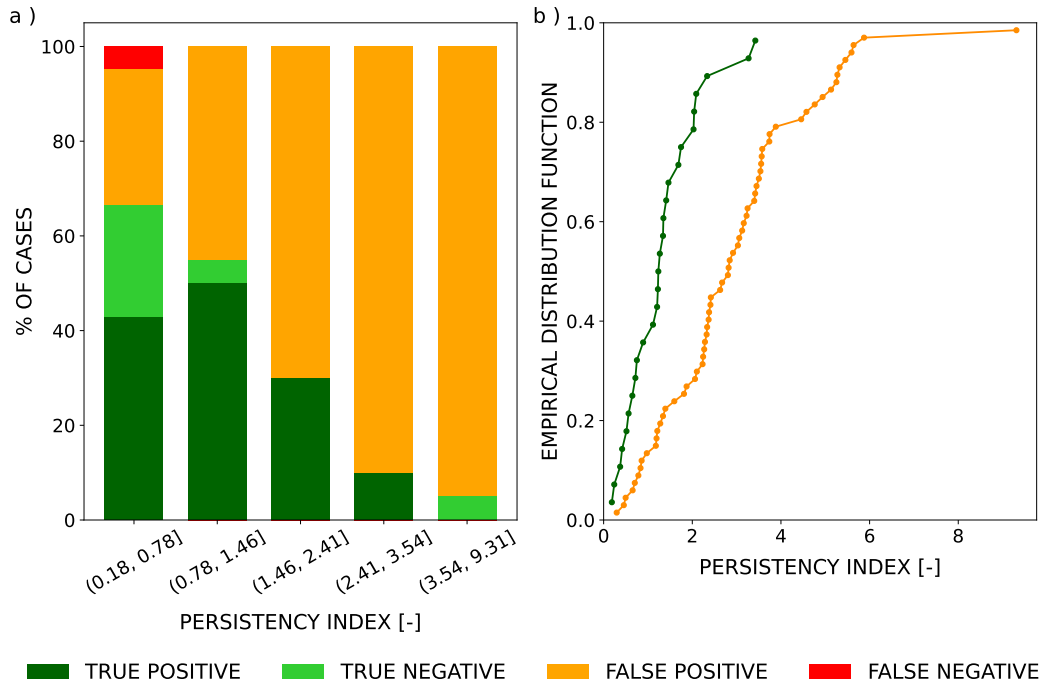


Figure 5: a) Performance of the PHysically-based Extreme Value (PHEV) distribution of river flows in the detection of flood divides as a function of the persistency index. Ranges (whose boundaries are reported in the x-axis) were set so as to have an equal number of values (~ 20) per bin. b) Empirical cumulative distribution functions of the persistency index for true positive (dark green) and false positive (orange) cases. The distributions are significantly different in a statistical sense (the p-value of the 2-samples Kolmogorov-Smirnov test is lower than 0.01.)

308 as such large events enabling detection of flood divides from empirical flood frequency curves
 309 are less likely to have been observed during the available data record.

310 Figure 5a displays the percentages of true positives (dark green color), true negatives
 311 (light green), false negatives (red) and false positives (orange) for five ranges of the per-
 312 sistency index set so as to have an equal number of values (~ 20) per bin. The number
 313 of false positives consistently increases with the persistency index, thus corroborating the
 314 above reasoning. No clear patterns are instead observed with, e.g., the drainage area and
 315 the average rainfall magnitude in the catchment (Figure S3), which are sometimes regarded
 316 as possible drivers of a marked increase of the magnitude of the rarer floods (Gaume, 2006;
 317 Villarini & Smith, 2010).

318 A recent review of the current scientific knowledge (B. Merz et al., 2022) suggests
 319 explanations for these results. It signals an unlikely direct role of catchment size in deter-
 320 mining tail behaviors of flood distributions, as increasing drainage areas entail both spatial

321 aggregation (which may cause lighter tails), and shifts of dominant processes (e.g., different
322 precipitation types and runoff generation mechanisms) which may lead in the opposite di-
323 rection. It also reports robust evidences against a dominant role of rainfall characteristics
324 for the emergence of heavy-tailed flood distributions, as runoff generation processes strongly
325 modulate the hydrologic response. On the contrary, the available literature emphasizes the
326 role of non-linear hydrological responses and the catchment water balance for the emergence
327 of heavy tails. These are the two key processes described by PHEV and summarized by the
328 persistency index, which thus arises as a pivotal indicator of the possibility to detect flood
329 divides from data records.

330 To further highlight the relation between typical river flow dynamics recapped in the
331 persistency index and the occurrence of false positives we compare in Figure 5b the cumu-
332 lative distributions of the persistency index for the sets of true positives (dark green) and
333 false positives (orange). The distributions clearly differ and false positives mostly occur
334 for persistent regimes. This qualitative evaluation is validated by applying the 2-sample
335 Kolmogorov-Smirnov test, which evaluates if two samples come from the same distribution
336 (null-hypothesis): in this case we can reject the null-hypothesis at the 0.01 significance level,
337 meaning that the two samples are drawn from different distributions and false positives are
338 significantly more likely to occur for persistent regimes. The same cannot be proved for the
339 cumulative distributions of catchment area (p-value = 0.44) and average rainfall magnitude
340 (p-value = 0.34) for the sets of true and false positives. Remarkably, the seasons charac-
341 terized by the larger portion of false positives are spring and winter, during which regimes
342 tend to be more persistent.

343 The physical explanation provided here of the different telling power of streamflow data
344 for rivers characterized by distinctively different streamflow dynamics agrees with the results
345 of previous research. For example, Botter et al. (2013) showed less variable streamflow
346 distributions across years in erratic regimes compared to persistent ones, which determines
347 higher representativeness of their estimates in the former case for a given length of the data
348 record. Smith et al. (2018) also demonstrated that upper tail ratios grow with the length
349 of data and, for a given data length, are larger (i.e., flood divides are more often identified)
350 in arid and semiarid regions than in humid ones. Their results jointly suggest that, given
351 similarly long data records, the typical (erratic) flow dynamics of drier areas enable more
352 reliable characterization of the whole range of values possibly spanned by streamflow and

353 of the presence or absence of flood divides according to the physical explanation provided
354 above.

355 **4 Concluding Remarks**

356 In this work we examine the occurrence of marked uprisers of flood frequency curves
357 (termed flood divides), which are pivotal for a correct estimation of river flood hazard. We
358 develop a robust methodology to identify them from observational records and models, and
359 evaluate the capability of the PHysically-based Extreme Value distribution of river flows
360 (PHEV) to reliably detect flood divides.

361 Results show that PHEV is consistently able to recognize the presence/absence of flood
362 divides in a large set of case studies from the US and Germany. Possible reasons for the
363 occurrence of a sizeable number of false positives are investigated by accounting for both
364 the statistical uncertainty of relatively short observational records and the typical hydro-
365 climatic variability of different river basins, which affects the information content of these
366 limited data series. To this end, we perform a controlled experiment in which we remove
367 the highest flow maxima in the flood frequency curves of the true positive cases and repeat
368 the flood divide detection analysis on the shorter series, showing that PHEV can foresee
369 the emergence of true flood divides in more than 80% of the cases even if the shortened
370 observations do not display them. The result supports claims of the dependability of flood
371 divides initially classified as false positives. An investigation of the intrinsic dynamics of
372 streamflows in the set of true and false positives further elucidates the issue. False positives
373 are indeed preferentially found for more persistent regimes (87% of the false positives have
374 persistency index above two, as opposed to only 11% of true positives; the overall number
375 of cases with persistency index above two is 55) which, by their nature, rarely exhibit large
376 extreme flow values. The limited length of the available observed time series might be thus
377 constraining the possibility to observe expected flood divides, analogously to what occurs
378 when we artificially reduce the size of the observational sample.

379 The present analysis, performed on a wide set of catchments characterized by different
380 hydroclimatic features, reveals PHEV as a reliable tool to identify and foresee the occurrence
381 of flood divides and consequently unveil the propensity of rivers to large floods. The method
382 is especially relevant in data scarce conditions, although limitations linked to the domain
383 of applicability of this tools exist and have been recalled in this work. The study lays

384 the foundations for a better comprehension of climate and landscape controls of observed
385 marked rises of the magnitude of the rarer floods, which is the subject of ongoing research.

386 **Acknowledgments**

387 This work is funded by the Deutsche Forschungsgemeinschaft (DFG, German Research
388 Foundation) - Project Number 421396820 'Propensity of rivers to extreme floods: climate-
389 landscape controls and early detection (PREDICTED)' and Research Group FOR 2416
390 'Space-Time Dynamics of Extreme Floods (SPATE)'. The financial support of the Helmholtz
391 Centre for Environmental Research - UFZ is as well acknowledged. We thank the Bavar-
392 ian State Office of Environment (LfU, <https://www.gkd.bayern.de/de/fluesse/abfluss>)
393 and the Global Runoff Data Centre (GRDC) prepared by the Federal Institute for Hy-
394 drology (BfG, <http://www.bafg.de/GRDC>) for providing the discharge data for Germany.
395 The MOPEX dataset is available at [https://hydrology.nws.noaa.gov/pub/gcip/mopex/
396 US_Data/](https://hydrology.nws.noaa.gov/pub/gcip/mopex/US_Data/). 30-year normal precipitation gridded data for the US are provided by the PRISM
397 Climate Group, Oregon State University, <http://prism.oregonstate.edu> (downloaded on
398 June, 1st 2021); 30-year normal precipitation gridded data for Germany are provided by
399 the Deutsche Wetter Dienst (DWD) at [https://opendata.dwd.de/climate_environment/
400 CDC/grids_germany/multi_annual/precipitation/](https://opendata.dwd.de/climate_environment/CDC/grids_germany/multi_annual/precipitation/)

401 **References**

- 402 Allamano, P., Laio, F., & Claps, P. (2011). Effects of disregarding seasonality on the
403 distribution of hydrological extremes. *Hydrol. Earth Syst. Sci.*, *15*, 3207–3215. doi:
404 doi:10.5194/hess-15-3207-2011
- 405 Baratti, E., Montanari, A., Castellarin, A., Salinas, J. L., Viglione, A., & Bezzi, A. (2012).
406 Estimating the flood frequency distribution at seasonal and annual time scales. *Hydrol.*
407 *Earth Syst. Sci.*, *16*, 4651-4660. doi: 10.5194/hess-16-4651-2012
- 408 Basso, S., Botter, G., Merz, R., & Miniussi, A. (2021). Phev! the physically-based extreme
409 value distribution of river flows. *Environ. Res. Lett.*, *16*, 124065. doi: 10.1088/
410 1748-9326/ac3d59
- 411 Basso, S., Frascati, A., Marani, M., Schirmer, M., & Botter, G. (2015). Climatic and
412 landscape controls on effective discharge. *Geophysical Research Letters*, *42*, 8441–8447.
413 doi: 10.1002/2015GL066014
- 414 Basso, S., Schirmer, M., & Botter, G. (2015). On the emergence of heavy-tailed streamflow

- distributions. *Advances in Water Resources*, *82*, 98 - 105. doi: 10.1016/j.advwatres
.2015.04.013
- Basso, S., Schirmer, M., & Botter, G. (2016). A physically based analytical model of flood
frequency curves. *Geophysical Research Letters*, *43*(17), 9070-9076. doi: 10.1002/
2016GL069915
- Berghuijs, W. R., Sivapalan, M., Woods, R. A., & Savenije, H. (2014). Patterns of similarity
of seasonal water balances: A window into streamflow variability over a range of time
scales. *Water Resources Research*, *50*, 5638 - 5661. doi: 10.1002/2014WR015692
- Bernardara, P., Schertzer, D., Eric, S., Tchiguirinskaia, I., & Lang, M. (2008). The flood
probability distribution tail: How heavy is it? *Stochastic Environmental Research and
Risk Assessment*, *22*, 5638 - 5661. doi: 10.1002/2014WR015692
- Biswal, B., & Marani, M. (2010). Geomorphological origin of recession curves. *Geophysical
Research Letters*, *37*(24). (L24403) doi: 10.1029/2010GL045415
- Botter, G., Basso, S., Rodriguez-Iturbe, I., & Rinaldo, A. (2013). Resilience of river flow
regimes. *Proceedings of the National Academy of Sciences*, *110*(32), 12925-12930. doi:
10.1073/pnas.1311920110
- Botter, G., Porporato, A., Rodriguez-Iturbe, I., & Rinaldo, A. (2007). Basin-scale soil mois-
ture dynamics and the probabilistic characterization of carrier hydrologic flows: Slow,
leaching-prone components of the hydrologic response. *Water Resources Research*,
43(2). doi: 10.1029/2006WR005043
- Botter, G., Porporato, A., Rodriguez-Iturbe, I., & Rinaldo, A. (2009). Nonlinear storage-
discharge relations and catchment streamflow regimes. *Water Resources Research*,
45(10). doi: 10.1029/2008WR007658
- Brutsaert, W., & Nieber, J. L. (1977, 6). Regionalized drought flow hydrographs from a
mature glaciated plateau. *Water Resources Research*, *13*(3), 637-643. doi: 10.1029/
WR013i003p00637
- Budyko, M. (1974). *Climate and life*. Academic Press.
- Cohen, J. (1974). *Statistical power analysis for the behavioral sciences*. Lawrence Erlbaum
Associates.
- Deal, E., Braun, J., & Botter, G. (2018). Understanding the role of rainfall and hydrology in
determining fluvial erosion efficiency. *Journal of Geophysical Research: Earth Surface*,
123(4), 744-778. doi: 10.1002/2017JF004393
- Duan, Q., Shaake, J., Andreassian, V., S., F., Goteti, G., Gupta, H., . . . Wood., E. (2005).

- 448 Model parameter estimation experiment (mopex): An overview of science strategy
449 and major results from the second and third workshops. *Journal of Hydrology*, 320,
450 3 - 17. doi: 10.1016/j.jhydrol.2005.07.031
- 451 Farquharson, F. A. K., Meigh, J. R., & Sutcliffe, J. (1992). Regional flood frequency
452 analysis in arid and semi-arid areas. *J. Hydrol.*, 138(3), 487-501. doi: 10.1016/
453 0022-1694(92)90132-F
- 454 Gaume, E. (2006). On the asymptotic behavior of flood peak distributions. *Hydrol. Earth*
455 *Syst. Sci.*, 10, 233-243.
- 456 Gignac, G. E., & Szodorai, E. T. (2016). Effect size guidelines for individual differences
457 researchers. *Personality and Individual Differences*, 102, 74-78. doi: 10.1016/j.paid
458 .2016.06.069
- 459 Guo, J., Li, H.-Y., Leung, L. R., Guo, S., Liu, P., & Sivapalan, M. (2014). Links be-
460 tween flood frequency and annual water balance behaviors: A basis for similarity and
461 regionalization. *Water Resources Research*, 50. doi: 10.1002/2013WR014374
- 462 Hirschboeck, K. (1987). Hydroclimatically-defined mixed distributions in partial dura-
463 tion flood series. In *In: Singh v.p. (eds) hydrologic frequency modeling* (p. 199-
464 212). Louisiana State University, Baton Rouge, U.S.A: Springer, Dordrecht. doi:
465 10.1007/978-94-009-3953-0_13
- 466 Jianchun, L., Pope, G. A., & Sepehrnoori, K. (1994). A high-resolution finite-difference
467 scheme for nonuniform grids. *Appl. Math. Modelling*, 19, 162 - 172.
- 468 Laio, F., Porporato, A., Ridolfi, L., & Rodriguez-Iturbe, I. (2001). Plants in water-controlled
469 ecosystems: active role in hydrologic processes and response to water stress: Ii. prob-
470 abilistic soil moisture dynamics. *Advances in Water Resources*, 24(7), 707 - 723. doi:
471 10.1016/S0309-1708(01)00005-7
- 472 Lovakov, A., & Agadullina, E. R. (2021). Empirically derived guidelines for effect size
473 interpretation in social psychology. *European Journal of Social Psychology*, 51(3),
474 485-504. doi: 10.1002/ejsp.2752
- 475 Mann, H. B., & Whitney, D. R. (1947). On a Test of Whether one of Two Random Variables
476 is Stochastically Larger than the Other. *The Annals of Mathematical Statistics*, 18(1),
477 50 - 60. doi: 10.1214/aoms/1177730491
- 478 Merz, B., Basso, S., Fischer, S., Lun, D., Blöschl, G., Merz, R., ... Schumann, A. (2022).
479 Understanding heavy tails of flood peak distributions. *Water Resources Research*,
480 58(6), e2021WR030506. doi: 10.1029/2021WR030506

- 481 Merz, B., Blöschl, G., Vorogushyn, S., & et al. (2021). Causes, impacts and patterns
482 of disastrous river floods. *Nat. Rev. Earth Environ.*, *2*, 592 – 609. doi: 10.1038/
483 s43017-021-00195-3
- 484 Merz, B., Vorogushyn, S., Lall, U., Viglione, A., & Blöschl, G. (2015). Charting unknown
485 waters — on the role of surprise in flood risk assessment and management. *Water*
486 *Resources Research*, *51*, 6399 – 6416. doi: 10.1002/2015WR017464
- 487 Merz, R., & Blöschl, G. (2003). A process typology of regional floods. *Water Resources*
488 *Research*, *39*, 9578 – 9591. doi: 10.1029/2002WR001952
- 489 Merz, R., Tarasova, L., & Basso, S. (2020). Parameter’s controls of distributed catchment
490 models—how much information is in conventional catchment descriptors? *Water*
491 *Resources Research*, *56*(2), e2019WR026008. doi: 10.1029/2019WR026008
- 492 Mushtaq, S., Miniussi, A., Merz, R., & Basso, S. (2022). Reliable estimation of high
493 floods: A method to select the most suitable ordinary distribution in the metasta-
494 tistical extreme value framework. *Advances in Water Resources*, *161*, 104127. doi:
495 10.1016/j.advwatres.2022.104127
- 496 Porporato, A., Daly, E., & Rodriguez-Iturbe, I. (2004). Soil water balance and ecosystem
497 response to climate change. *The American Naturalist*, *164*, 625–632. doi: 10.1086/
498 424970
- 499 Rogger, M., Pirkl, H., Viglione, A., Komma, J., Kohl, B., Kirnbauer, R., ... Blöschl, G.
500 (2012). Step changes in the flood frequency curve: process controls. *Water Resources*
501 *Research*, *48*, W05544. doi: 10.1029/2011WR011187
- 502 Rogger, M., Viglione, A., Derx, J., & Blöschl, G. (2013). Quantifying effects of catchments
503 storage thresholds on step changes in the flood frequency curve. *Water Resources*
504 *Research*, *49*, 6946–6958. doi: 10.1002/wrcr.20553
- 505 Schaake, J., Duan, Q., Andréassian, V., Franks, S., Hall, A., & Leavesley, G. (2006). The
506 model parameter estimation experiment (mopex). *Journal of Hydrology*, *320*(1), 1 -
507 2. (The model parameter estimation experiment) doi: 10.1016/j.jhydrol.2005.07.054
- 508 Smith, J. A., Cox, A. A., Baeck, M. L., Yang, L., & Bates, P. D. (2018). Strange floods:
509 The upper tail of flood peaks in the united states. *Water Resources Research*, *54*,
510 6510-6542. doi: 10.1029/2018WR022539
- 511 Sullivan, G., & Feinn, R. (2012). Using effect size — or why the p value is not enough.
512 *Journal of Graduate Medical Education*, 279-282. doi: 10.4300/JGME-D-12-00156.1
- 513 Tarasova, L., Basso, S., & Merz, R. (2020). Transformation of generation processes

514 from small runoff events to large floods. *Geophysical Research Letters*, 47(22),
515 e2020GL090547. doi: 10.1029/2020GL090547

516 Tarasova, L., Basso, S., Zink, M., & Merz, R. (2018). Exploring controls on rainfall-runoff
517 events: 1. Time series-based event separation and temporal dynamics of event runoff
518 response in Germany. *Water Resources Research*, 54, 7711 - 7732. doi: 10.1029/
519 2018WR022587

520 Villarini, G., & Smith, J. (2010). Flood peak distributions for the eastern united states.
521 *Water Resources Research*, 46. doi: 10.1029/2009WR008395

522 Wallemacq, P., & House, R. (2018). *Economic Losses, Poverty & Disasters 1998-2017* (Tech.
523 Rep.). United Nations Office for Disaster Risk Reduction (UNDRR) and Centre for
524 Research on the Epidemiology of Disasters (CRED).

525 Wang, D., & Hejazi, M. (2011). Quantifying the relative contribution of the climate and
526 direct human impacts on mean annual streamflow in the contiguous United States.
527 *Water Resources Research*, 47. doi: 10.1029/2010WR010283